Macromolecules in ordered media: 1. Interfacial interactions between a cationic polymer and oppositely charged liposomes

Iolanda Porcar, Clara M. Gómez, Enrique Pérez-Payá*, Vicente Soria and Agustín Campos†

Departament de Química Física, Universitat de València, E-46100 Burjassot, València, Spain

(Received 26 July 1993; revised 1 March 1994)

The incorporation of a cationic polymer, such as poly(4-vinylpyridine), to the outer leaflet of negatively charged phospholipid vesicles of dimyristoylphosphatidic acid has been investigated by viscometry and intrinsic fluorescence. Viscosity changes of dilute solutions follow the size of the polymer and the polymer–liposome complex. Variations in the emission spectrum of poly(4-vinylpyridine) upon the addition of lipid vesicles under different conditions give the amount of polymer bound per mole of accessible lipid. These experimental results have been interpreted by means of the Gouy–Chapman formalism, which calculates the effective number of charges per polymer chain at the interface. The size of the adsorbed polyion has been computed from a discrete charge virial expansion that takes into account the mobility of charged groups at the interface.

(Keywords: fluorescence; liposomes; poly(4-vinylpyridine))

INTRODUCTION

There is a growing interest for the macromolecular and colloid chemist[1,2] in the study of interactions between polymers and amphiphilic aggregates as a key to the behaviour of biological assemblies. Many papers[3–7], theoretical, as well as experimental, have been devoted to explaining how interactions occur between polymer chains and colloidal particles, whereas few studies have been published on polymer–liposome interactions. For example, Klimov and Khohlov[8] have recently studied the formation of a complex between a polymer chain and colloidal particles using scaling arguments. McQuigg *et al.*[2] have analysed the conditions for the binding of polyelectrolytes to small oppositely charged micelles, while Raudino and coworkers[9–11] have proposed a theoretical model for studying the interaction between charged lipid vesicles and an electrolyte solution containing hydrophilic nonionic polymers. Thomas and Tirrell[12] have studied how the use of polyelectrolytes can control the organization of phospholipid bilayers.

The molecular interactions of charged polymers with oppositely charged lipid vesicles or liposomes in aqueous solution are strongly dependent on the ionic strength, pH, chemical structure, number of charges, etc., and their mechanism involves a combination of electrostatic and hydrophobic effects[13]. A similar type of electrostatic interaction between small charged molecules, such as drugs, hormones, peptides or proteins, and lipid bilayers has been investigated intensively[14–20] in attempts to model the incorporation of these molecules to a membrane in biological media. These interactions are experimentally represented by a binding isotherm, and can be semiquantitatively interpreted by combining a simple partition equilibrium with the Gouy–Chapman model for charged surfaces[20]. Whereas this formalism has been extensively applied to the association of peptides to lipid vesicles[18–23], no similar work has been found in the literature for charged polymers interacting with liposomes.

The aim of this work is to explore the behaviour of a vinyl cationic polymer adsorbed at the outer lipid bilayer. A system formed by poly(4-vinylpyridine) (P4VPy), which has fluorescent properties, and lipid vesicles of dimyristoylphosphatidic acid (DMPA) in acetate buffer has been chosen. The size of the polymer and of the polymer–liposome complex structure which is formed upon interaction have been determined by viscometry. The same technique has been used to detect possible conformational changes of the polymer as a function of temperature. In this context, a methodology which is similar to that often used to describe the association of amphiphilic peptides and unilamellar vesicles has been followed[19]. To attain this goal, binding curves corresponding to the partition equilibrium of the polymer between the lipid and aqueous phases, have been determined by intrinsic fluorescence experiments. An activity coefficient has been introduced in the original formalism to correct for the polymer concentration. Two expressions, derived from the Gouy–Chapman[19] and virial[20] approaches, have been used to obtain the effective charge and the radius of the polymer at the interface, respectively.

*Permanent address: Departament de Bioquímica i Biologia Molecular, Universitat de València, E-46100 Burjassot, València, Spain
† To whom correspondence should be addressed

0032-3861/94/21/4627–11
© 1994 Butterworth-Heinemann Ltd

EXPERIMENTAL

Materials

Dimyristoylphosphatidic acid (DMPA) was purchased from the Sigma Chem. Co. (St. Louis, MO, USA) and poly(4-vinylpyridine) (P4VPy), with a molecular weight (M_w) of 50 000, from Polysciences Inc. (Warrington, PA, USA). Both materials were used without further purification.

For the viscometry and fluorescence measurements, the following buffer was used: 20 mM sodium acetate, 0.18 M acetic acid (ionic strength, $c_s = 0.0266$ M; pH = 3.5), and 1 mM EDTA. Under these experimental conditions, P4VPy is fully protonated and the lipid vesicles bear a negative charge for each phospholipid head.

Preparation of lipid samples for viscosity and fluorescence experiments

Small unilamellar vesicles (SUV) of DMPA were prepared as follows: according to the final concentration required, a quantity from 11 to 22 mg of DMPA was dissolved in a mixture of benzene/methanol (2:1, by volume), evaporated in a round-bottomed flask by the use of a rotary evaporator for at least 45 min at 70°C, and then put under a stream of dry nitrogen. The dried lipid film was then dissolved in the appropriate volume of buffer solution, heated up to 60°C (above the transition temperature of DMPA) for 10 min and shaken gently on a vortex mixer. The hydrated lipid dispersion was then sonicated for a specific time, depending on the total volume used (1 min ml^{-1}), to promote the formation of unilamellar liposomes. Large unilamellar vesicles (LUV) (pellet) were removed from the SUV (supernatant) by centrifugation (using a Beckman Microfugue TM) for 10 min at 12 000 rev min^{-1}.

Viscometry

The viscosity measurements were made with a conventional Ubbelohde capillary viscometer (Model AVS 440, from Schott–Gerate, Germany). This instrument determines the elution times automatically. For each solution, a 15 ml sample was loaded into the viscometer, which was then placed into a thermostated bath at different temperatures (5, 22, 30, 35, 40, 50, 55 and 70 ± 0.01°C). Measurements were started after an equilibration time of ~5–10 min, and were continued until several of the elution time readings agreed to within 0.5%. The capillary sizes were selected so that kinetic energy corrections were minimal.

The samples used to measure the viscosity of the P4VPy–lipid vesicles were prepared by adding to a solution containing 3 mM of lipid and 2.5 μM of P4VPy different volumes of a solution of 2.5 μM of polymer in acetate buffer, in order to achieve different lipid-to-polymer molar ratios, R_i, ranging from 120 to 2, as in the fluorescence experiments (see below).

Fluorescence measurements

The association of P4VPy to the DMPA vesicles was monitored by intrinsic fluorescence experiments, using a Perkin–Elmer Model LS-5B Luminescence Spectrometer equipped with a 3700 Data Station, carried out at five different temperatures, namely 5, 20, 37, 56 and 76°C, with the latter controlled by a TU3-S8 Lauda Thermostat. Fluorescent samples were obtained by mixing a solution of P4VPy with 2 ml of lipid vesicles of the required concentrations so as to obtain the selected R_i ratios.

RESULTS

Viscometry

Figure 1 shows the dependence of the reduced viscosity $\eta_{sp}/[P_T]$ (where η_{sp} refers to the specific viscosity of P4VPy and $[P_T]$ to its total concentration) on $[P_T]$ at different temperatures, T, covering the range from 5 to 70°C. At temperatures from 5 to 35°C, the reduced viscosity decreases as the polymer concentration is lowered; similar behaviour has been observed for solutions of polyelectrolytes at moderate ionic strength[24–27]. However, at temperatures ranging from 40 to 70°C, $\eta_{sp}/[P_T]$ increases with a decrease in polymer concentration. The opposite behaviour of the reduced viscosity as a function of $[P_T]$ when increasing T can be related to a conformational transition of the P4VPy molecules by means of the viscosimetric interaction parameter. A conformational transition has been previously reported for poly(2-vinylpyridine), which is based on a discontinuity in the unperturbed dimension parameter K_θ, in the long-range interaction parameter B (from the Stockmayer–Fixman plot[28]) and in the preferential solvation parameter of the polymer[29]. In a similar way, for P4VPy we observed that at $[P_T] > 2 \times 10^{-4}$ g ml^{-1} plots of the reduced viscosity against $[P_T]$ (*Figure 1*) are linear and

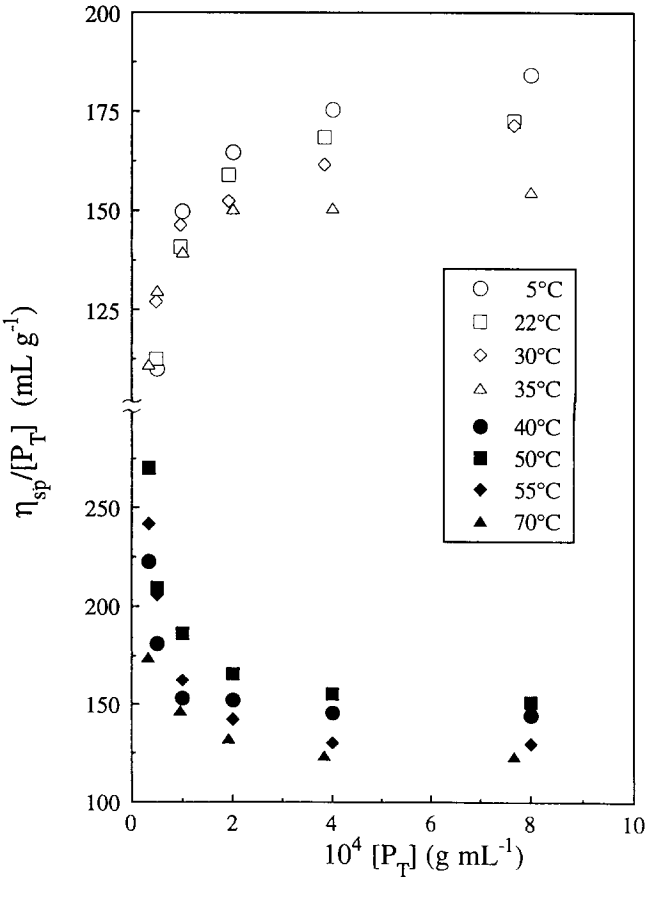

Figure 1 Plot of the reduced viscosity of poly(4-vinylpyridine), $\eta_{sp}/[P_T]$, as a function of the total polymer concentration, $[P_T]$, at different temperatures

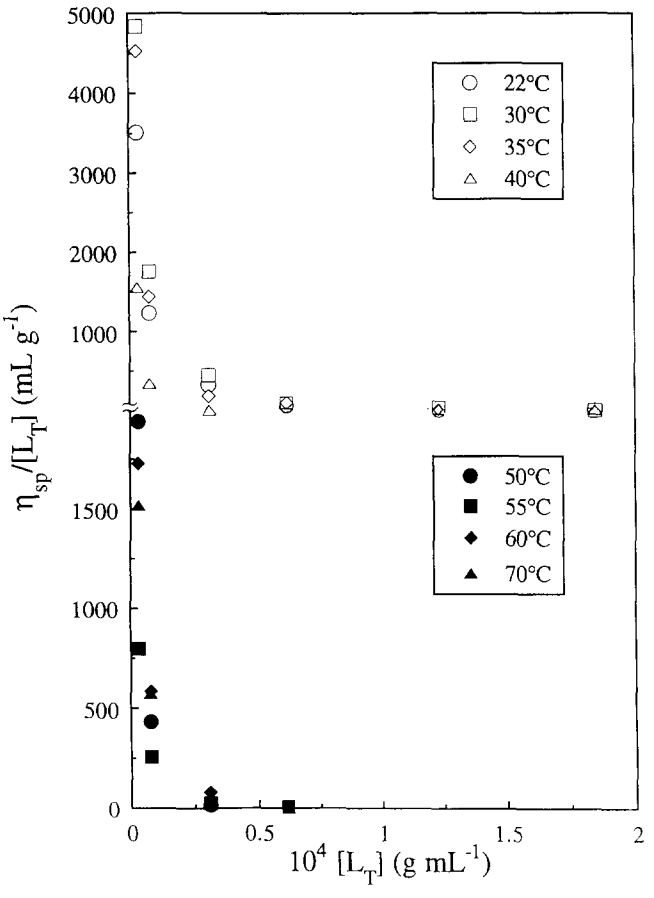

Figure 2 Plot of the reduced viscosity of phospholipid vesicles, $\eta_{sp}/[L_T]$, in buffered solutions (2.5 μM) of poly(4-vinylpyridine) as a function of the total lipid concentration, $[L_T]$, at different temperatures

fit the well known Huggins equation[30], with a slope which equals b, the viscometric interaction parameter between the polymer segments. Then, from the plot of the reduced viscosity, we obtain a change in b from positive ($T = 5$–$35°C$) to negative ($T = 40$–$70°C$). A conformational transition has been directly related to a discontinuity in K_θ[29,31], but an abrupt decrease in this parameter coincides with a rapid increase in B. Moreover, although the two parameters b and B are obtained from different viscosity plots, they both represent polymer–solvent interactions. Therefore, the change in b that is observed for P4VPy could be attributed to a conformational transition which is related to the existence of two ordered structures of the polymer chain, which result from different inter- and intramolecular interactions among the polymer segments.

Figure 2 shows the plot of $\eta_{sp}/[L_T]$ against $[L_T]$ in aqueous solutions of acetate buffer (where η_{sp} refers to the specific viscosity of the DMPA vesicles in the presence of P4VPy, with $[P_T] = 2.5\,\mu M$, and $[L_T]$ to the total concentration of DMPA), at different temperatures, ranging from 22 to 70°C. In this figure, a typical polyelectrolyte behaviour[24–27] is observed, with an increase in the reduced viscosity as the liposome concentration is lowered. The reduced viscosity of the liposomes in the presence of P4VPy is ~10–25 times higher than that of the polymer alone, which is possibly due to the formation of a DMPA vesicles–P4VPy complex. The polymer chain is adsorbed on the lipid vesicles, with some of its segments in direct contact with the lipid surface, while the others form loops joining two vesicles, with a consequent increase in the hydrodynamic volume and the reduced viscosity.

In order to elucidate the possible proportion of the reduced viscosity of the lipid vesicles to the hydrodynamic volume, a fact that has been widely corroborated with neutral and charged synthetic polymers[32,33], the Einstein–Simha equation[34], i.e. $\eta_{sp} = \mu V_h N_0 [L_T]/[L_T]_0$, has been used. Here, μ is a proportionality constant that depends on the spheroidal axial ratio of the lipid vesicle, V_h is the hydrodynamic particle volume, N_0 is the initial number of liposomes per millilitre of sample, and $[L_T]_0$ and $[L_T]$ are the concentrations of lipid sample at the start and after successive dilution, respectively. *Figure 3a* shows the plot of η_{sp} against $[L_T]/[L_T]_0$ for DMPA vesicles at 22°C. In contrast to a similar plot for asolectin liposomes[35], the plot of the Einstein–Simha equation[34] (*Figure 3a*) does not fit a straight line, but the slope decreases with an increase of liposome concentration up to a constant value; hence, V_h changes with $[L_T]$. *Figure 3b* shows the plot of the same viscosity data as in *Figure 3a*, but in this case in the form of $\eta_{sp}/[L_T]$ against $[L_T]$. The reduced viscosity decreases to a constant value as the lipid concentration increases, as is usually observed for polyelectrolyte solutions[24–27]. *Figure 3b* shows a minimum in $\eta_{sp}/[L_T]$ at $[L_T] \sim 2 \times 10^{-4}$ g ml^{-1}, although

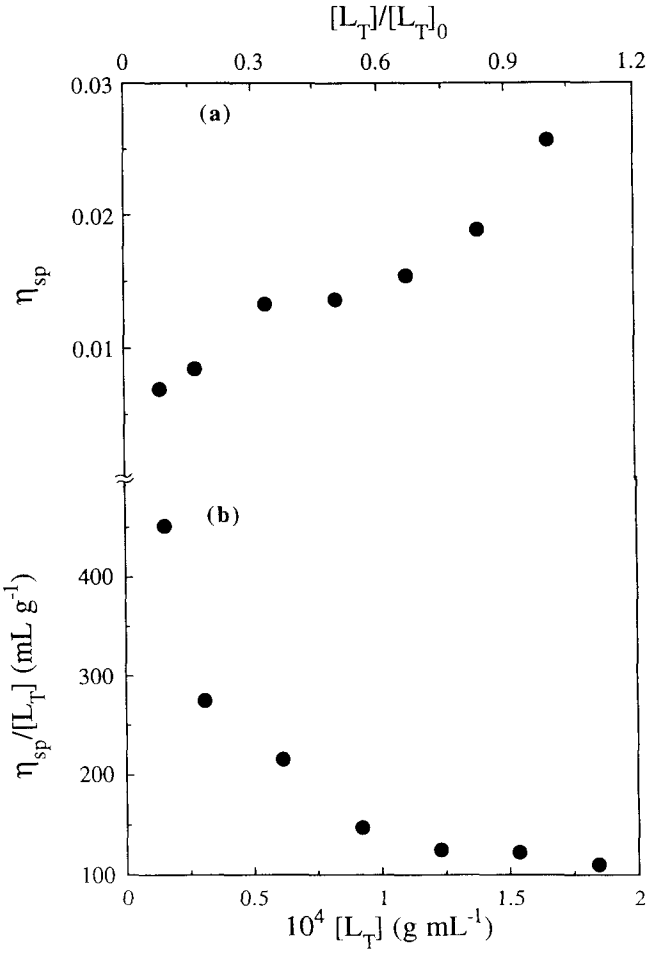

Figure 3 (a) Specific viscosity of phospholipid vesicles, η_{sp}, as a function of the ratio of lipid concentration, $[L_T]/[L_T]_0$, at 22°C and (b) total lipid concentration, $[L_T]$, dependence on the liposomes reduced viscosity, $\eta_{sp}/[L_T]$, at 22°C

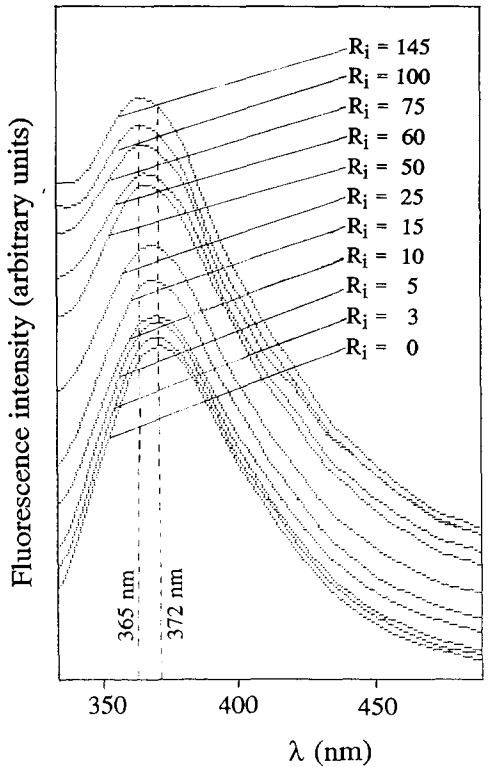

Figure 4 Typical fluorescence spectra of poly(4-vinylpyridine) in buffer solution ($c_s = 0.0266$ M, pH = 3.5) as a function of the lipid-to-polymer molar ratio, R_i, at $T = 20°C$; the excitation wavelength was set at 305 nm

the maximum value cannot be detected. At high lipid concentrations, the lipid vesicles come close together and overlap one another, thus preventing the superficial negative charges from repelling each other, with a consequent reduction of V_h. However, at low $[L_T]$ values, repulsion between the superficial negative charges of the liposomes will enhance V_h. By comparing *Figures 3a* and *3b*, the proportionality between the reduced viscosity and V_h can be derived. From *Figure 3a*, at low liposome concentrations (lc) it holds that: $[L_T]/[L_T]_0 = 0.08$, $\eta_{sp} = 0.007\ \text{ml g}^{-1}$, and the Einstein–Simha equation gives $(V_hN)^{lc} = 0.003$, i.e., up to 0.3% of the total volume is occupied by liposomes. However, at high concentrations (hc), $[L_T]/[L_T]_0 = 1$, $\eta_{sp} = 0.026\ \text{ml g}^{-1}$ and $(V_hN)^{hc} = 0.011$, i.e. 1.1% of the total volume is occupied by liposomes. The ratio of V_hN at low and high concentrations therefore gives:

$$(V_hN)^{lc}/(V_hN)^{hc} = (0.08V_h^{lc}N_0)/(1V_h^{hc}N_0) = 0.27$$

where this expression can be simplified to give the ratio of the hydrodynamic volumes, $V_h^{lc}/V_h^{hc} = 3.40$. From *Figure 3b*, we can also calculate the ratio between the $\eta_{sp}/[L_T]$ values at the same concentrations, i.e. $(\eta_{sp}/[L_T])^{lc}/(\eta_{sp}/[L_T])^{hc} = 3.80$, where this relationship yields the same numerical factor as that previously obtained. Therefore, we can conclude that $\eta_{sp}/[L_T]$ is proportional to V_h, and an increase or decrease of $\eta_{sp}/[L_T]$ implies the same change in V_h. We could reach the same conclusion by assuming that the plot of *Figure 3a* is linear over all of the liposome concentration range.

Fluorescence

In order to investigate the interaction of the fluorescent polymer molecule, P4VPy, on phospholipid vesicles, the changes in the intrinsic fluorescence as a function of ionic strength, lipid-to-polymer molar ratio, R_i, and temperature, have been followed. In particular, this technique has proved very useful in describing how interactions occur between small molecules, such as peptides and model lipid vesicles[36–39]. Changes in the wavelength of the emission maximum, $\Delta\lambda$, and in the fluorescence intensity, $\Delta I/I_0$ ($\Delta I = I - I_0$, where I_0 and I are the fluorescence intensities of pure P4VPy, and at a molar ratio R_i, respectively) will give information on the amount of this interaction.

As an example, *Figure 4* shows the fluorescence spectrum of P4VPy (5 μM) in the presence of increasing amounts of DMPA lipid vesicles (with different R_i ratios), at 20°C. The intrinsic fluorescence of the pyridine group is very sensitive to its binding to the phospholipids, with the wavelength of the emission maximum shifting from 372 to 365 nm as the lipid-to-polymer molar ratio R_i increases, indicating that the pyridine group is going from a polar to a non-polar environment, with a simultaneous increase in the fluorescence intensity. These changes are depicted in *Figures 5a* and *5b*, where the dependence of $\Delta\lambda$ and of $\Delta I/I_0$ on R_i at 372 nm is plotted as a function of temperature. Similar fluorescence results can be found in the literature[40–42] for peptide-lipid vesicles systems, although a plateau is found (all of the peptides present in solution being bound to lipids) at $R_i = 4$–100, depending on the pH and temperature. We need much higher values of R_i to reach a plateau (representing full binding) because we are dealing here with a synthetic polymer (P4VPy) with one positive charge for each monomer group,

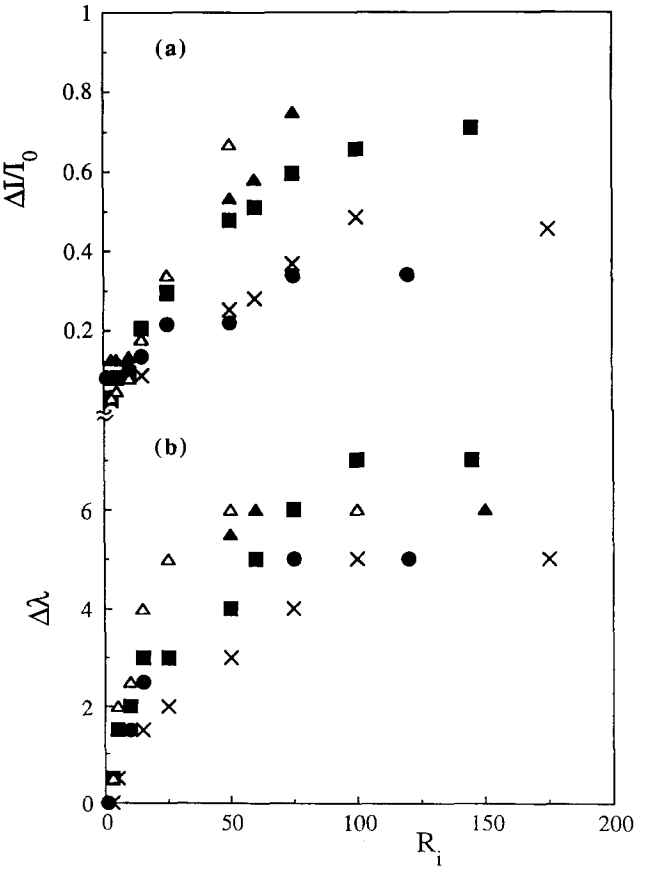

Figure 5 Influence of the temperature on the relative fluorescence intensity, $\Delta I/I_0$, at $\lambda = 372$ nm as a function of the lipid-to-polymer molar ratio, R_i, (a), and on the apparent wavelength shift of the maximum emission, also plotted as a function of R_i (b): (×) 5; (■) 20; (●) 37; (▲) 56 and (△) 76°C

whereas the peptides previously studied are small molecules, with each of them displaying ~5 or 6 positive charges.

DISCUSSION

Binding of a polymer to negatively charged phospholipid vesicles

As a first stage, the association of a positively charged polymer to negatively phospholipid membranes can be described by a binding equilibrium between the free polymer, P, and a membrane site formed by N charged lipids, S_N. This chemical model has recently been used to study the association of peptides with a phospholipid bilayer[29]. By assuming that the membrane sites are independent and equivalent binding sites, a rapid adsorption equilibrium may operate:

$$P + S_N \rightleftarrows PS_N \tag{1}$$

with an association constant:

$$K_A = \frac{[PS_N]}{[P][S_N]} \tag{2}$$

where $[PS_N]$ is the concentration of polymer bound to N membrane sites. The concentration of free membrane sites, $[S_N]$, and of free polymer, $[P]$, can be expressed as a function of the molar fraction of the occupied polymer binding sites, $\alpha = [PS_N]/[P_T]$, as follows:

$$[S_N] = [S_T] - [PS_N] = [S_T] - \alpha[S_T] = \frac{[L_T]}{N}(1-\alpha) \tag{3}$$

and

$$[P] = [P_T] - [PS_N] = [P_T] - \alpha[P_T] \tag{4}$$

with $[S_T] = [L_T]/N$ being the total concentration of membrane sites. The number of occupied membrane sites is usually small when compared to the number of free membrane sites, i.e. $[PS_N] \ll [S_N]$, and so we find that $[S_N] \approx [S_T]$.

The concentration of the two types of polymer, namely free and that bound to liposomes, can be experimentally determined from changes in the intrinsic fluorescence measurements. Therefore, the fluorescence intensity I at a molar ratio $R_i = [L_T]/[P_T]$ can be expressed as:

$$I = I_0 \frac{[P]}{[P_T]} + I_m \frac{[PS_N]}{[P_T]} \tag{5}$$

where I_0 and I_m are the fluorescence intensities of pure P4VPy and of P4VPy at lipid saturation, respectively, and $[P_T] = [PS_N] + [P]$. Equation (5) can be rearranged as follows:

$$\alpha = \frac{[PS_N]}{[P_T]} = \frac{I - I_0}{I_m - I_0} = \frac{\Delta I}{I_m - I_0} \tag{6}$$

On the other hand, the extent of binding, α/R_i, can be defined as the (molar) amount of polymer bound per mole of total lipid. For calculation reasons, and since the polymer is considered to only have access from outside the vesicle[19,23], α/R_i is corrected by the fraction of lipid, β, in the outer leaflet, as follows:

$$\frac{\alpha}{R_i^*} = \left(\frac{\alpha}{R_i}\right) \Big/ \beta \tag{7}$$

where α/R_i^* is the molar amount of polymer bound per mole of accessible liquid. For small unilamellar vesicles, such as the ones being considered in this present study, where nearly two-thirds of the lipids stay in the outer shell, β is 0.65[20].

By substituting equations (3), (4), and (7) into equation (2) and rearranging, the extent of binding can be expressed as:

$$\frac{\alpha}{R_i^*} = \frac{[P_T](1-\alpha)}{(K_A^{-1} + [P_T](1-\alpha))N} \tag{8}$$

The plot of α/R_i^* against the free polymer concentration $(1-\alpha)[P_T]$ should yield a straight line passing through the origin, where the slope is as follows:

$$\frac{\alpha[P_T]}{[L_T]\beta[P]} = \frac{K_A[S_N]}{[L_T]\beta} = \frac{K_A R_i^*/N[P_T]}{[L_T]\beta} = \frac{K_A}{N} \tag{9}$$

The physical meaning of this slope is the change in the number of moles of absorbed polymer, per mole of accessible lipid, with polymer concentration, i.e., it resembles a partitioning of the polymer between the lipid and aqueous phases, and should remain constant with temperature and pressure.

Figure 6 shows the association isotherms, α/R_i^* against $(1-\alpha)[P_T]$, for DMPA lipid vesicles with P4VPy ($[P_T] = 1.25$, 2.50, 3.75 and 5.00 μM) in aqueous acetate buffer solution at different temperatures, namely 5, 20, 37, 56, and 76°C. We obtain a different association isotherm for every $[P_T]$ and T value, and each one of these can be divided into two zones: (1) at high R_i^* values (low α/R_i^*), a nearly horizontal binding curve is obtained, with a deviation from the ideal straight line passing through the origin (see equation (8)), similar to that obtained by other authors when studying the association of peptides to lipid vesicles[18-23]; for region (2) there is a sharp increase of α/R_i^* at sufficiently low R_i^* values, and this sudden increase has only previously been observed for succinylated melittin with dimyristoylphosphatidyl choline (DMPC) lipid[36-38] at 30°C (0.1 M NaCl, pH = 7), and has been attributed to the formation of aggregates in the bilayer phase. By studying the variations in the binding curves when the temperature changes, it is noticed that at 5, 20 and 37°C, the binding curves show an increase in the extent of binding, α/R_i^*, as $[P_T]$ increases, whereas at higher temperatures, the opposite situation occurs. We will refer later to these binding curves with relationship to different parameters.

The partition equilibrium

In order to explain the deviation of the binding curves from the straight lines predicted by the chemical equilibrium (see equation (8)), it seems most appropriate to choose a partitioning approach which implies that the polymer becomes dissolved in the lipid bilayer as a result of favourable solvation effects exerted by the lipid. In this model, we consider two phases where the polymer can be found: one phase is formed by the lipid vesicles and the other is the aqueous solution. The partition coefficient, K_r, of polymer between the two phases, assuming that the polymer incorporation takes place without electrostatic interactions, can be defined as:

$$K_r = \frac{n_p^L/V_L}{n_p^A/V_A} \tag{10}$$

where n_p^L and n_p^A are the number of moles of polymer in the aqueous and lipid phases, respectively, with a total

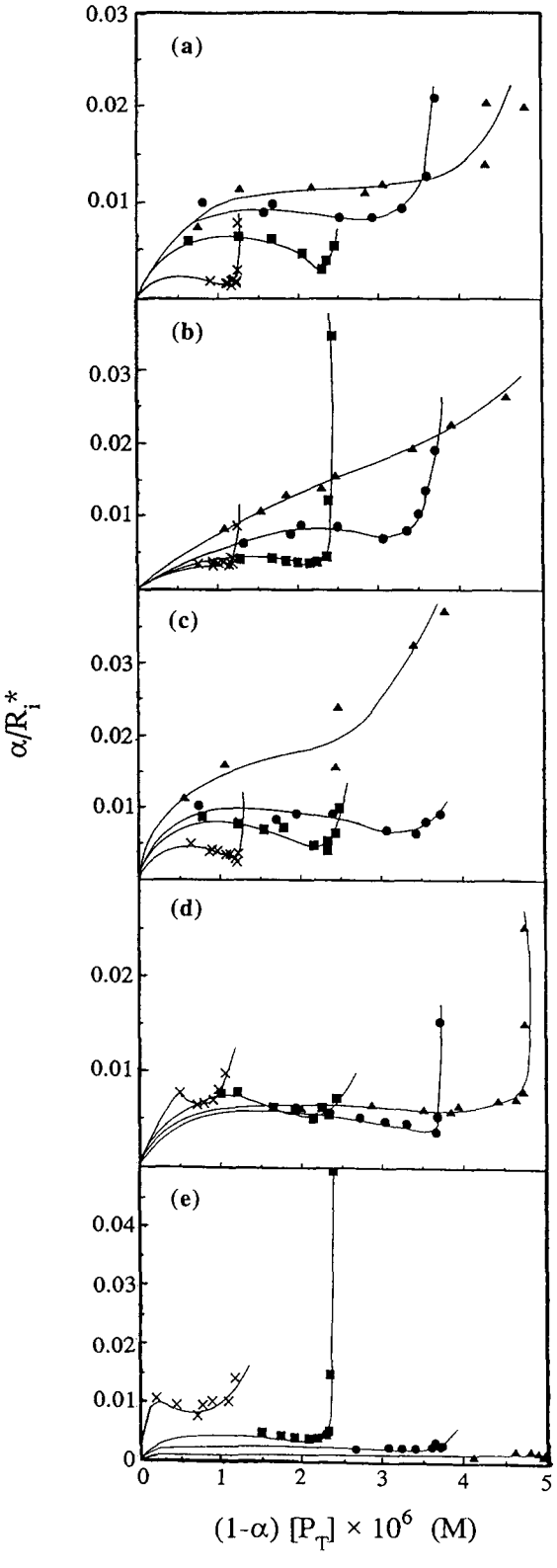

Figure 6 Binding isotherms of P4VPy to DMPA lipid vesicles obtained at different temperatures: (a) 5; (b) 20; (c) 37; (d) 56; (e) 76°C. Points denote the total P4VPy concentration $[P_T]$: (×) 1.25; (■) 2.50; (●) 3.75; (▲) 5.00 μM

number of moles of polymer, $n_p = n_p^L + n_p^A$. V_L and V_A are the respective volumes of the lipid and aqueous phase. The raw experimental data contains the total polymer $[P_T]$ and total lipid $[L_T]$ concentrations in the total volume V_T, although under most of the experimental conditions, the lipid concentration is very small, $[L_T] < 1$ mM. Therefore, we can consider that $V_T \approx V_A$, and hence:

$$K_r = \frac{n_p^L/V_L}{n_p^A/V_T} = \frac{n_p^L/V_L}{[P]} = \frac{n_p^L}{\bar{v}_L n_L [P]} = \frac{n_p^L/V_T}{\bar{v}_L [P] n_L/V_T} = \frac{[PS_N]}{\bar{v}_L [P][L_T]} \quad (11)$$

where $\bar{v}_L$ is the partial molar volume of the lipid, and n_L is the number of moles of lipid. The concentrations, $[PS_N]$ and [P] can be determined from fluorescence experiments, and therefore by substituting equations (4) and (6) into equation (11) it holds that:

$$\frac{\alpha}{R_i^*} = K_r \bar{v}_L (1-\alpha)[P_T] \quad (12)$$

The association isotherm will be governed by equation (12) on the basis that an ideal incorporation of polymer into the two phases takes place, and that the binding curves (*Figure 6*) should be straight lines passing through the origin, with a constant slope which is independent of the free polymer concentration and equal to $K_r \bar{v}_L$. However, this situation is not likely to occur, and the slope changes with [P], a fact that can be explained by assuming that the charge accumulation at the interface would reduce the polymer adsorption as a result of repulsive interactions that can be written in terms of an activity coefficient, γ. This electrostatic solute–solute repulsion gives rise to thermodynamically non-ideal effects, and therefore, a real partition equilibrium can be expressed as[19]:

$$\frac{\alpha}{R_i^*} = \frac{\Gamma}{\gamma}(1-\alpha)[P_T] \quad (13)$$

This expression involves a partition coefficient that is independent of polymer concentration, i.e. $\Gamma = K_r \bar{v}_L$, which is determined by the free energy difference of the substrate between the two media, and an activity coefficient, γ, that reflects possible non-ideal polyion–polyion interactions. The fact that we observed a pronounced curvature in the association isotherm with gradually decreasing values of the apparent partition coefficient, $\Gamma^{app} = \Gamma/\gamma$ (at least for low and moderate concentrations of the free polymer), suggests the existence of repulsive interactions between the repeating unit which is associated to both the liposomes and the free polymer in the aqueous solution. These interactions have also been observed in systems that are formed by small peptide molecules associated to lipid vesicles, and have been attributed to the electrostatic repulsion of a positively charged peptide, such as melittin[21–23]. A strict thermodynamic analysis of the adsorption equilibrium gives $\gamma = \gamma_P^L/\gamma_P^A$, where γ_P^L and γ_P^A refer to the activity coefficients of the polymer in the lipid and in the aqueous phase, respectively. However, the polymer concentration in the aqueous phase is very small: we can therefore consider that $\gamma_P^A \sim 1$, and so $\gamma = \gamma_P^L$, as used in this present paper. In a future work, a more detailed study of the coefficient γ_P^A, and its influence on the prediction of the binding curves, will be considered.

If adsorption of a positively charged polymer occurs at the interface which is composed of negatively charged lipid head groups, a theoretical expression for the activity coefficient can be derived by using the Gouy–Chapman approach for modelling charged surfaces[19]:

$$\ln \gamma = 2v \sinh^{-1}\left(vb' \frac{\alpha}{R_i^*} + b' z_{lip} x_{lip}\right) \quad (14)$$

where the parameter v stands for the effective number of charges per polymer chain at the interface and $b' = e^2/(2A_{lip}\kappa\varepsilon\varepsilon_0 kT)$, which is a constant for each temperature and equals $329.42\,T^{-1/2}$ for the experimental conditions of this paper (e is the electronic charge, A_{lip} is the molecular area of the lipid, $\kappa = (2e^2 c_s N_A/(\varepsilon\varepsilon_0 kT))^{1/2}$, i.e. the inverse Debye length, ε is the dielectric constant, ε_0 is the permittivity of vacuum and kT is the thermal energy). In addition, z_{lip} is the valency of the lipid head group and x_{lip} is the mole fraction of the charged over the total lipid.

Equations (13) and (14) are used to fit the experimental association isotherms with two free parameters: the partition coefficient Γ, which is related to the initial slope of the curves, and the effective interfacial charge, v, which is related to the degree of binding. We have calculated the parameter Γ by fitting the experimental data to equations (13) and (14) for the lowest polymer concentration, $[P_T] = 1.25\,\mu M$, and a temperature, $T = 5°C$ (*Figure 6a*). The parameter v has been previously obtained by assuming that at low values of T and $[P_T]$ the total persistence length of the charged polymer, L_T, is directly proportional to the temperature[43]. The reduced viscosity, which is proportional to the polyion hydrodynamic radius, R_h[44], decreases with decreasing T and polyion concentration (see *Figure 1*). Therefore, under these experimental conditions, the polymer obtains a rod-like conformation, a larger proportion of the polymer chain remains at the lipid interface and a maximum value for v is reached. By assuming that P4VPy ($M_w = 50\,kDa$) is fully protonated under the above conditions, with one positive charge per repeat unit, we obtain $v = 490$. Using this value and the experimental data of *Figure 6a*, an average value of $\Gamma = 7.7 \times 10^4\,M^{-1}$ is obtained, which is similar to those obtained for the partition equilibrium of melittin between the aqueous and lipid phases[21]. A unique value of $\Gamma = 7.7 \times 10^4\,M^{-1}$ for every association curve has been used in this paper, supported by the fact that when Γ is increased up to $4 \times 10^{10}\,M^{-1}$, a variation in v of only $\sim 5\%$ is observed. In order to calculate the values of v by equation (14), the γ data were previously obtained from equation (13) by using the experimental data of the association isotherms (*Figure 6*) with $\Gamma = 7.7 \times 10^4\,M^{-1}$. *Table 1* summarizes the mean average v values thus obtained for the two zones of the isotherms. For the first zone, these values show different trends in T and $[P_T]$, i.e. from 5 to 56°C, v decreases as $[P_T]$ increases, whereas from 56 to 76°C, an increase in v is observed. This behaviour can be correlated with the dependence of the reduced viscosity on $[P_T]$ between 5 and 35°C (*Figure 1*); the reduced viscosity increases with $[P_T]$ and so does the hydrodynamic volume, probably due to a diminution of the segment fraction by polymer chains at the interface, quantitatively represented by a reduction in the v values. The opposite situation occurs from 40 to 70°C, showing a decrease in the reduced viscosity with $[P_T]$. On the other hand, the v values show different trends when changing the polymer concentration: at low $[P_T]$, e.g. $1.25\,\mu M$, v decreases as T increases, at high $[P_T]$, e.g. $5.00\,\mu M$, v increases as T increases, while at medium $[P_T]$, e.g. $2.5\,\mu M$, v decreases from 5 to 56°C and then increases again. In order to analyse this behaviour, *Figure 7* shows plots of $\eta_{sp}/[P_T]$ and v against T for different values of $[P_T]$. Under every condition, an opposite dependence of $\eta_{sp}/[P_T]$ and v on T is observed, i.e. a decrease of $\eta_{sp}/[P_T]$ implies that a greater density of polymer segments (by volume) can

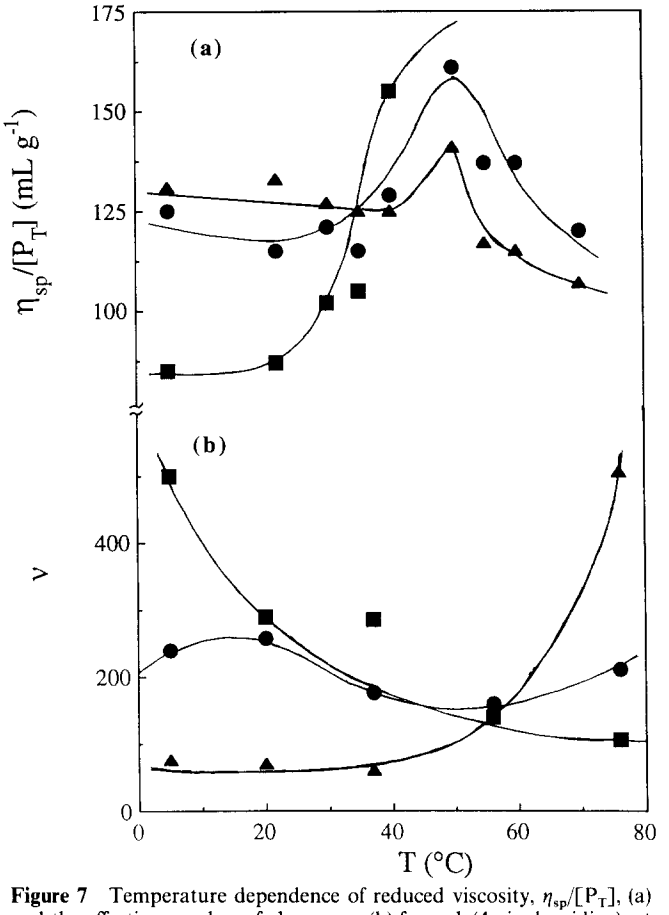

Figure 7 Temperature dependence of reduced viscosity, $\eta_{sp}/[P_T]$, (a) and the effective number of charges, v, (b) for poly(4-vinylpyridine), at different total polymer concentrations: (■) 1.25; (●) 2.50; (▲) 5.00 μM

Table 1 Effective number of charges per polymer chain at the interface, v, calculated by fitting the binding curves (*Figure 6*) to equations (13) and (14) with $\Gamma = 7.7 \times 10^4\,M^{-1}$, at different total polymer concentrations and temperatures

T (°C)	$[P_T]^a$ (μM)				$[P_T]^b$ (μM)			
	1.25	2.50	3.75	5.00	1.25	2.50	3.75	5.00
5	500±100	240±90	107±10	77±7	230±100	180	62±15	49±1
20	290±20	258±20	119±23	71±21	176±60	54±20	62±10	40±3
37	286±48	176±62	124±29	61±1	199±75	145±45	115±7	27±2
56	140±13	160±33	188±28	154±15	111	138	125±60	81±42
76	107±18	212±3	326±55	506±76	68	42±24		

[a] Values obtained for the first zone of the isotherm (see *Figure 6*)
[b] Values obtained for the region of the isotherm where an abrupt increase of α/R_i^* is observed (see *Figure 6*)

Table 2 Polyion radii R obtained at 20°C by fitting equation (A5) (see Appendix) to the experimental activity coefficient calculated with the aid of equation (13) and the binding curves (*Figure 6*), for different values of the total polymer concentration $[P_T]$, as a function of the extent of binding α/R_i^*

$[P_T]$ (μM)	α/R_i^* ($\times 10^3$)	R (Å)	$[P_T]$ (μM)	α/R_i^* ($\times 10^3$)	R (Å)	$[P_T]$ (μM)	α/R_i^* ($\times 10^3$)	R (Å)	$[P_T]$ (μM)	α/R_i^* ($\times 10^3$)	R (Å)
1.25	3.21	8.34	2.5	4.21	13.36	3.75	7.6	24.19	5.00	10.7	30.0
1.25	3.66	10.80	2.5	3.89	11.93	3.75	8.8	26.96	5.00	12.9	34.3
1.25	3.55	10.21	2.5	3.68	10.88	3.75	8.6	26.52	5.00	13.8	35.6
1.25	3.68	10.89	2.5	3.59	10.41	3.75	7.0	22.78	5.00	15.5	36.9
1.25	3.28	8.78	2.5	3.77	11.32	3.75	8.0	25.31	5.00	19.3	42.2
1.25	3.41	9.45	2.5	4.49	14.53	3.75	10.3	30.05	5.00	22.5	45.5
1.25	4.20	13.31	2.5	12.10	33.10	3.75	13.5	35.22	5.00	26.5	48.8
1.25	8.61	26.65	2.5	34.90	55.94	3.75	19.1	42.00			

Table 3 Polyion radii R obtained at 37°C by fitting equation (A5) (see Appendix) to the experimental activity coefficient calculated with the aid of equation (13) and the binding curves (*Figure 6*), for different values of the total polymer concentration $[P_T]$, as a function of the extent of binding α/R_i^*

$[P_T]$ (μM)	α/R_i^* ($\times 10^3$)	R (Å)	$[P_T]$ (μM)	α/R_i^* ($\times 10^3$)	R (Å)	$[P_T]$ (μM)	α/R_i^* ($\times 10^3$)	R (Å)	$[P_T]$ (μM)	α/R_i^* ($\times 10^3$)	R (Å)
1.25	3.89	12.24	2.5	8.82	24.89	3.75	10.32	26.95	5.00	16.14	39.85
1.25	4.18	13.61	2.5	7.73	25.34	3.75	8.42	26.99	5.00	15.76	39.34
1.25	4.04	12.96	2.5	7.00	23.44	3.75	9.24	28.78	5.00	24.00	48.30
1.25	3.51	10.32	2.5	7.29	24.21	3.75	9.22	28.75	5.00	32.53	55.97
1.25	3.58	10.69	2.5	4.83	16.36	3.75	6.98	23.38	5.00	37.23	60.75
1.25	2.98	9.22	2.5	4.12	13.32	3.75	6.51	22.05			
1.25	3.64	10.98	2.5	5.42	18.55	3.75	8.15	26.36			
1.25	7.98	25.98	2.5	6.51	22.04	3.75	9.23	28.78			
			2.5	9.98	30.28						

approach the outer leaflet bilayer, thus increasing the v values.

For the second zone of the isotherm, the sudden decrease in v where an abrupt increase of α/R_i^* is observed, can also be attributed to changes in the reduced viscosity of the liposomes (see *Figures 3* and *4*) in the presence of P4VPy. In this way, for low values of $[L_T]$, $\eta_{sp}/[L_T]$ shows the highest numerical values, indicating that the size of the lipid vesicle increases sharply. The attractive force of the polymer towards the lipid head is reduced, and so a smaller proportion of the polymer segments at the outer face per polymer chain causes a diminution of the v values, as can be seen from *Table 1*.

The other model which is used to correlate the activity coefficient with the parameters involved in the polymer–lipid interface is based on the virial approach[20]. Details of the calculation of the master equation generated by this approach, and which is used here, are given in the Appendix.

The experimental R values obtained by the virial approach have been calculated from equation (A5) (see Appendix), with the γ values being evaluated by following the same procedure as used above. Values of R, obtained by solving equation (A5) by a Newton–Raphson algorithm, are compiled in *Tables 2* and *3*, as a function of $[P_T]$, at 20 and 37°C, respectively. For every isotherm, the mean average R value shows a nearly constant value at low α/R_i^* values, with a sudden increase at high α/R_i^* values, whereas they increase with $[P_T]$ at a constant temperature, and with temperature at a constant $[P_T]$. The variation of R with both $[P_T]$ and T follows the same trend as that observed for v and the reduced viscosity, i.e. an increase of R is observed with an increase in the reduced viscosity, and by a reduction in the interfacial charge, the density of segments (by volume) is found to decrease.

Surface charge density and surface potential

The effective charge of the polymer bound to the lipid vesicle, according to the Gouy–Chapman formalism, is considered to be smeared uniformly over the outer leaflet of the DMPA vesicle; therefore, an electric surface charge density, σ, can be generated[22,23] and is calculated by using the following[18]:

$$\sigma = \left(ve \frac{\alpha}{R_i^*} \Big/ A_{lip} \right) \Big/ \left(1 + \frac{A_p}{A_{lip}} \right) \quad (15)$$

where A_p/A_{lip} is a factor used to correct for the expansion of the lipid surface upon polymer binding. For low α/R_i^* coverage, the influence of the correction is negligible and equation (15) can be approximated to the following:

$$\sigma = ve \frac{\alpha}{R_i^*} \Big/ A_{lip} \quad (16)$$

In addition, the surface charge at the lipid surface generates a surface potential, Ψ_0, which can be calculated by means of the Gouy–Chapman theory[46]:

$$\sigma^2 = 2000 \varepsilon_0 \varepsilon RT \sum_i c_i [\exp(-z_i F_0 \Psi_0 / RT) - 1] \quad (17)$$

where c_i and z_i are the concentration of the ith electrolyte in the bulk aqueous phase and the signed valency of the ith species, respectively, and F_0 is the Faraday constant ($F_0 = 96\,486\ \mathrm{C\,mol^{-1}}$). *Table 4* summarizes the σ and Ψ_0 values which have been calculated with the aid of

Table 4 Electric surface charge density σ and surface potential Ψ_0 at 5°C, calculated by using equations (16) and (17), respectively, for different values of the total polymer concentration $[P_T]$, as a function of the extent of binding α/R_i^*

$[P_T]$ (μM)	α/R_i^* ($\times 10^3$)	σ (C m^{-2})	Ψ_0 (mV)	$[P_T]$ (μM)	α/R_i^* ($\times 10^3$)	σ (C m^{-2})	Ψ_0 (mV)	$[P_T]$ (μM)	α/R_i^* ($\times 10^3$)	σ (C m^{-2})	Ψ_0 (mV)	$[P_T]$ (μM)	α/R_i^* ($\times 10^3$)	σ (C m^{-2})	Ψ_0 (mV)
1.25	1.58	0.236	114.14	2.5	6.41	0.234	113.99	3.75	10.06	0.231	113.68	5.00	11.5	0.231	113.70
1.25	1.56	0.236	114.15	2.5	6.17	0.235	114.04	3.75	8.96	0.233	113.90	5.00	11.6	0.233	113.85
1.25	1.32	0.236	114.15	2.5	4.69	0.235	114.11	3.75	9.86	0.233	113.87	5.00	11.1	0.234	113.95
1.25	1.82	0.236	114.14	2.5	3.02	0.236	114.16	3.75	8.45	0.234	114.02	5.00	12.0	0.234	113.93
1.25	1.95	0.236	114.14	2.5	3.92	0.236	114.15	3.75	8.47	0.235	114.05	5.00	14.0	0.234	113.96
1.25	1.57	0.236	114.15	2.5	5.45	0.235	114.10	3.75	9.39	0.235	114.05	5.00	20.3	0.231	113.71
1.25	1.77	0.236	114.15						12.78	0.234	113.95	5.00	19.8	0.232	113.76
1.25	2.93	0.235	114.12						20.79	0.230	113.60				

equations (16) and (17), respectively, for the binding of P4VPy to DMPA liposomes at 5°C. Similar results have also been obtained at temperatures of 20, 37, 56 and 76°C. These calculated values are positive and constant for each binding curve, with a fairly steady increase of Ψ_0 with T.

The effect of the surface potential is to repel polymer ions from the lipid surface, thus hindering them from approaching. Therefore, the polyion concentration immediately above the plane of binding, $[P]^{corr}$, will be lower than the concentration in the bulk solution, [P], with[22] $[P]^{corr} = [P]\exp(-v\Psi_0 F_0/RT)$. By assuming that an ideal incorporation of polymer into the two phases takes place, these two concentrations can be related through the partition coefficient (see equation (12)) of polymer between the bulk and lipid phases, i.e. $\Gamma = K_r\bar{v}_L = \alpha/(R_i^*[P])$, and the partition coefficient of polymer between the plane close to the binding plane and the lipid phase, namely $\Gamma^{corr} = K_r^{corr}\bar{v}_L = \alpha/(R_i^*[P]^{corr})$. Taking into account the above assumptions, it holds that:

$$\frac{\Gamma}{\Gamma^{corr}} = \frac{K_r}{K_r^{corr}} = \frac{[P]^{corr}}{[P]} = \exp(-v\Psi_0 F_0/RT) \quad (18)$$

For $P_T = 1.25\,\mu$M at 20°C, we obtain the following: $\Gamma^{corr} = \Gamma\exp(v\Psi_0 F_0/RT) = \Gamma(6.81 \times 10^{38})$. So we can conclude that $K_r^{corr} \gg K_r$, as a result of electrostatic repulsions.

We can relate these results with previous studies on the interactions between peptides and lipid vesicles. For example, when a peptide, such as melittin modified by the introduction of monodansylcadaverine, interacts with SUV of egg yolk phosphatidyl choline (EPC), at pH 7, the following results are obtained: $v = 3.1$, $\sigma \sim 0.008$ C m^{-2}, and $\Psi_0 \sim 20$ mV. When the interaction takes place with SUV of dipalmitoyl phosphatidylcholine at 50°C, values of $v = 1.15$, $\sigma \sim 0.019$ C cm^{-2}, and $\Psi_0 \sim 45$ mV, are found[39]. By comparing these results with those obtained in this present study on the interaction of P4VPy with lipid vesicles of DMPA (*Table 4*), it is noticed that larger values of v, σ and Ψ_0 are obtained when dealing with a polymer molecule than with the comparatively small peptide molecules. Hence, although entropic effects hinder the polymer from approaching close to the outer lipid bilayer, the electrostatic interactions between P4VPy and the DMPA liposomes are stronger than when we consider small molecules, such as peptides, interacting with lipid vesicles.

In order to widen our understanding (at a molecular level) of the phenomena discussed here, more experimental, as well as theoretical investigations, are currently in progress.

CONCLUSIONS

The interactions between poly(4-vinylpyridine) (P4VPy) and dimyristoylphosphatidic acid (DMPA) vesicles have been studied by viscometry and intrinsic fluorescence, as a function of both polymer concentration and temperature, in aqueous media. Interpretation of the P4VPy viscosity measurements made in acetate buffer allow us to state that a charged form exists in this medium, which is probably the protonated form of the pyridine ring of the polymer, as a result of the acidity of the buffer. In addition, the variation in the reduced viscosity with temperature from 5–70°C (*Figure 1*) induces a change in its general trend as a function of polymer concentration close to 35–40°C, which can be attributed to a conformational change of the P4VPy coils. The curves obtained from viscosity measurements of the phospholipid solutions (*Figure 2*) follow the same pattern as seen in *Figure 1*, but the viscosity changes become more pronounced when increasing the lipid concentration. The viscosity decrease reflects the screening of charges on the solute (polymer or phospholipid), thus resulting in a more flexible chain. Correlations between the viscosity data and the hydrodynamic volume of the liposomes has been established by using the well known Simha–Einstein equation (*Figure 3a*), because in this context diminution of the viscosity reveals an overall reduction in the hydrodynamic volume. Considering these arguments, the electrostatic nature of the interaction, as well as changes in the overall size of the polymer and of the polymer–vesicle complex, have been demonstrated.

To allow a more precise interpretation, it is necessary to understand how this interaction takes place. For this reason, intrinsic fluorescence experiments on polymer–lipid vesicles mixtures, carried out at different polymer concentrations and covering a wide temperature range, have been performed. The shift of the emission peak wavelength (see *Figures 4* and *5*) has demonstrated how the presence of the lipid vesicle, when positioned close to the polymer, affects the fluorescence of the pyridine ring. Fluorescence experiments allow quantitative determination of the degree of binding by means of the association isotherms, which show distinct patterns with changes in the total polymer concentration and temperature (*Figure 6*). Each of these isotherms shows two zones: for the first zone, the degree of binding remains

almost constant, or slightly decreases, while for the second zone, a sharp increase in this parameter is observed.

These experimental data have been interpreted by both Gouy–Chapman and virial treatments, as applied to solutions of macromolecular solutes which are adsorbed to charged walls. The effective number of charges per polymer chain at the interface v, has been calculated by the Gouy–Chapman approach and gives values which are less than the physical charge. The radius, R, of the polyion adsorbed at the interface, which has been obtained from the virial formalism, has been related to the reduced viscosity and with the v values. An increase in v is supported by the fact that both R and the reduced viscosity decreases (*Figure 7*), showing that a smaller fraction of the polymer segments can approach the outer bilayer leaflet. In addition, the surface charge density and surface potential have been calculated and it has been found that the numerical values obtained are much greater than those found for the interaction of peptides with small unilamellar vesicles.

ACKNOWLEDGEMENTS

This work was partly funded by the Comision Interministerial de Ciencia y Tecnologia (Spain), Grant No. PB91-0808. One of us, I. Porcar, is indebted to the Ministerio de Educación y Ciencia (Spain) for a Fellowship grant.

REFERENCES

1 Jiulin, X., Dubin, P. L. and Kim, Y. *J. Phys. Chem.* 1992, **96**, 6805
2 McQuigg, D. W., Kaplan, J. I. and Dubin, P. L. *J. Phys. Chem.* 1992, **96**, 1973
3 Goddard, E. D. *Colloids Surf.* 1986, **19**, 255
4 Thalberg, K., Lindman, B. and Karlstrom, G. *J. Phys. Chem.* 1990, **94**, 4289
5 Dubin, P. L., The, S. S., Gan, L. M. and Chew, C. H. *Macromolecules* 1990, **23**, 2500
6 Nagarajan, R. *J. Chem. Phys.* 1989, **90**, 1980
7 Laroche, G., Dufourc, E. J., Pézolet, M. and Dufourcq, J. *Biochemistry* 1990, **29**, 6460
8 Klimov, D. K. and Khokhlov, A. R. *Polymer* 1992, **33**, 2177
9 Raudino, A. and Castelli, F. *Macromolecules* 1992, **25**, 1594
10 Raudino, A. and Bianciardi, P. *J. Theor. Biol.* 1991, **149**, 1
11 Raudino, A., Catelli, F. and Gurrieri, S. *J. Phys. Chem.* 1990, **94**, 1526
12 Thomas, J. L. and Tirrell, D. A. *Acc. Chem. Res.* 1992, **25**, 8
13 Sargent, D. F. and Schwyzer, R. *Proc. Natl. Acad. Sci. USA* 1986, **83**, 5774
14 McLaughlin, S. and Harary, H. *Biochemistry* 1976, **15**, 1941
15 Lee, A. G. *Biochim. Biophys. Acta* 1978, **514**, 95
16 Seelig, A., Allegri, P. R. and Seelig, J. *Biochim. Biophys. Acta* 1988, **939**, 267
17 Seelig, A. and McDonald, P. *Biochemistry* 1989, **28**, 2490
18 Beschiaschvili, G. and Seelig, J. *Biochemistry* 1990, **29**, 52
19 Schwarz, G. and Beschiachvili, G. *Biochim. Biophys. Acta* 1989, **979**, 82
20 Stankowski, S. *Biophys. J.* 1991, **60**, 341
21 Stankowski, S. and Schwarz, G. *Biochim. Biophys. Acta* 1990, **1025**, 164
22 Beschiaschvili, G. and Baeuerle, H.-D. *Biochim. Biophys. Acta* 1991, **1068**, 195
23 Kuchinka, E. and Seelig, J. *Biochemistry* 1989, **28**, 4216
24 Ganter, J. L. M. S., Milas, M. and Rinaudo, M. *Polymer* 1992, **33**, 113
25 Cohen, J. and Priel, Z. *Macromolecules* 1989, **22**, 2356
26 Cohen, J., Priel, Z. and Rabin, Y. *J. Chem. Phys.* 1988, **88**, 7111
27 Cohen, J. and Priel, Z. *J. Chem. Phys.* 1990, **93**, 9062
28 Stockmayer, W. and Fixman, M. *J. Polym. Sci.* 1963, **1**, 137
29 Vira, F., Viras, K., Aroni, F. and Dondos, A. *Eur. Polym. J.* 1974, **10**, 891
30 Bohdanecky, M. and Kovar, J. in 'Viscosity of Polymer Solutions' (Ed. A. D. Jenkins), Elsevier, Amsterdam, 1982, p. 176
31 Dondos, A. *Makromol. Chem.* 1972, **162**, 113
32 Figueruelo, J. E., Campos, A., Soria, V. and Tejero, R. *J. Liq. Chromatogr.* 1984, **7**, 1061
33 Soria, V., Garcia, R., Campos, A., Braco, L. and Abad, C. *Br. Polym. J.* 1988, **20**, 115
34 Schurz, J. 'Struktur-Rheologie', Berliner Union, Stuttgart, 1974
35 Nordmeier, E., Zeilinger, C. and Lechner, M. D. *J. Appl. Polym. Sci.* 1992, **44**, 533
36 Vogel, H. *FEBS Lett.* 1981, **134**, 37
37 Bernard, E., Faucon, J. F. and Dufourcq, J. *Biochim. Biophys. Acta* 1982, **688**, 152
38 Thiaudière, E., Siffert, O., Talbot, J. C., Bolard, J., Alouf, J. E. and Dufourcq, J. *Eur. J. Biochem.* 1991, **195**, 203
39 Pèrez-Payà, E. *PhD Thesis*, University of Valencia, Spain, 1992
40 Alouf, J. E., Dufourcq, J., Siffert, O., Thiaudière, E. and Geoffroy, C. *Eur. J. Biochem.* 1989, **183**, 381
41 Dufourcq, J. and Faucon, J. F. *Biochim. Biophys. Acta* 1977, **467**, 1
42 Bernard, E., Faucon, J. F. and Dufourcq, J. *Biochim. Biophys. Acta* 1982, **688**, 152
43 Hodgson, D. F. and Amis, E. J. in 'Polyelectrolytes' (Ed. M. Hara), Marcel Dekker, New York, 1993, p. 152
44 Hodgson, D. F. and Amis, E. J. in 'Polyelectrolytes' (Ed. M. Hara), Marcel Dekker, New York, 1993, p. 160
45 Hill, T. 'Introduction to Statistical Thermodynamics', Addison Wesley, Reading, MA, 1960, p. 261
46 Mclaughlin, S. *Curr. Top. Membrane Transport* 1977, **9**, 71
47 Stankowski, S. *Biochim. Biophys. Acta* 1983, **735**, 353
48 Stankowski, S. *Biochim. Biophys. Acta* 1984, **777**, 167
49 Trauble, H. and Eibl, H. in 'Functional Linkage in Biomolecular Systems' (Eds. F. O. Schmitt, D. M. Scheinder and D. M. Grothers), Raven Press, New York, 1971, p. 59

APPENDIX

Calculation of the size of the absorbing polyions by using the virial approach

By analogy to binary mixtures of real gases[45], a virial approach has been extended to the case of adsorbed polymer at charged bilayers. In this context, the activity coefficient of the adsorbed species, P4VPy in our case, can be expressed as[20]:

$$\ln \gamma = 2B_2(\text{rep})\frac{\alpha}{R_i^*} + 2B_2(\text{att})x_{\text{lip}} \qquad \text{(A1)}$$

where B_2(rep) refers to the repulsive pair interaction between the polymer chains, and B_2(att) to the attractive pair interaction between the adsorbing species and the lipid head groups. We shall restrict this model to shapes that are circularly symmetric at the interface, by considering an extreme case in which the z-valent charge remains point-like but is surrounded by a disc-shaped belt of radius R. Using this assumption, the second virial coefficient can be written as[20]:

$$B_2 = \frac{2\pi R^2}{A_{\text{lip}}} + \frac{\pi}{A_{\text{lip}}}\int_{2R}^{\infty} [1-\exp(-U(r)/kT)]r\,dr \qquad \text{(A2)}$$

where the first term is the excluded-area contribution that gives the entropic effect due to steric exclusion[47,48], and R is the polyion radius. If R is large enough, $U(r)$ will remain $\ll kT$ over the complete integration range; the exponential can then be expanded and the integral solved analytically, yielding:

$$B_2 = \frac{2\pi R^2}{A_{\text{lip}}} + z^2 b' \exp(-2\kappa R) \qquad \text{(A3)}$$

Using this expression in equation (A1), the activity

coefficient becomes:

$$\ln\gamma = \frac{\alpha}{R_i^*}\left[\frac{4\pi R^2}{A_{lip}} + 2z^2 b' \exp(-2\kappa R)\right] + \frac{4\pi R'^2}{A_{lip}} + 2z z_{lip} b' \exp(-2\kappa R') \quad \text{(A4)}$$

by assuming that $x_{lip}=1$. It is well known that phosphatidic acid can give rise to two dissociation equilibria, corresponding to the loss of one or two protons by the phosphate group, with pK_a values of ~ 3 and 8.5, respectively[49]. Therefore, at a pH of 3.5, the lipid bears only one negative charge, and $z_{lip}=-1$. On the other hand, we take $2R$ as the distance of closest approach of the two adsorbate macromolecules and $2R'$ as a distance of closest approach which is equal to the addition of the individual radii for the adsorbate and for the lipid head group. As the radii of the lipid head group is negligibly small when compared to the polyion radii, we can assume that $2R' \approx R$, and so finally we obtain the following:

$$\ln\gamma = \frac{\alpha}{R_i^*}\left[\frac{4\pi R^2}{A_{lip}} + 2z^2 b' \exp(-2\kappa R)\right] + \frac{\pi R^2}{A_{lip}} - 2z b' \exp(-\kappa R) \quad \text{(A5)}$$

Equation (A5) gives the activity coefficient as developed from the virial approach by incorporating the finite size of the adsorbing macroions through R, the polyion radius.